

PAPER

[View Article Online](#)
[View Journal](#)

Cite this: DOI: 10.1039/d5dt02303c

Structural diversity in Zn(II)/Cu(II) complexes with salicylic/acetylsalicylic acids and bis(4-pyridylthio) methane: coordination polymers, one organic cocrystal, and one organic salt

Olaya Gómez-Paz, ^{a,b} Rosa Carballo, ^{a,b} Ana B. Lago, ^{*c} Ezequiel M. Vázquez-López ^{a,b} and Berta Covelo^d

The solid-state chemistry of Zn(II)/Cu(II) salts with salicylic and acetylsalicylic acids and bis(4-pyridylthio) methane (SCS) was explored using various synthetic methods, leading to the isolation of several crystalline materials. These included three polymorphic forms of the one-dimensional coordination polymer $\frac{1}{\infty}\text{Zn}(\text{Hsal})_2(\text{SCS})$ (**1m**, **1m'** and **1o**), as well as the hydrated pseudopolymorph $\frac{1}{\infty}\text{Zn}(\text{Hsal})_2(\text{SCS})\cdot\text{H}_2\text{O}$ (**1w**). Additionally, a two-dimensional polymer $\frac{2}{\infty}\text{Cu}(\text{Hsal})_2(\text{SCS})\cdot\text{CH}_3\text{CN}$ (**2-CH₃CN**), a three-dimensional salicylate polymer $\frac{3}{\infty}\text{Cu}_5(\text{Hsal})_6(\text{sal})_2(\text{SCS})_4(\text{H}_2\text{O})_2$ (**4-solv**), and a two-dimensional aspirinate polymer $\frac{2}{\infty}\text{Cu}_3(\text{CH}_3\text{CO}_2)_4\text{asp}_2(\text{SCS})_3(\text{H}_2\text{O})_2$ (**3-solv**), which also contain a coordinated acetate anion, were obtained. In most systems, the crystallization of the organic salt $[(\text{H-SCS})(\text{Hsal})]$ (**5**) and the organic cocrystal $[(\text{SCS})(\text{H}_2\text{sal})_2]$ (**6**) was also observed. All materials were structurally characterized. Stability studies of compound **1m** were conducted in water, under acidic conditions and in physiological PBS buffer. Furthermore, the cytotoxicity of the zinc polymorphic polymers was evaluated against non-tumoral human cells (MRC-5) and tumour cell lines (NCI-H460, A549 and MDA-MB231).

Received 26th September 2025,
Accepted 31st October 2025

DOI: 10.1039/d5dt02303c

rsc.li/dalton

Introduction

Bioactive organic molecules, such as drugs and biomolecules, contain functional groups (carboxylate, phenol, thiol, heterocyclic nitrogen, *etc.*) that can act as ligands towards metal cations to form metal complexes. The coordination chemistry of these molecules may have some biological and pharmacological implications, for example in metalloenzymes mimicking biological functions or in metallodrugs with enhanced drug activity. Metallodrugs, like other metal complexes, can exhibit sensitivity to various stimuli like pH changes, light exposure, ion activation, or redox conditions so that they could result in efficient systems for the controlled release of a certain drug.¹ In this field, coordination polymers are currently attractive host materials for drug incorporation.^{2,3}

Among bioactive organic ligands are salicylates, highlighting salicylic acid (H_2sal) which is the principal metabolite of

acetylsalicylic acid (Aspirin®, Hasp) and responsible for the anti-inflammatory, antipyretic and analgesic effects of aspirin. On the other hand, salicylic acid and salicylates are naturally present in various plants, fruits, vegetables and spices and it has been suggested that a diet rich in these compounds helps to reduce the risk of suffering from some diseases such as colorectal cancer.⁴ In addition, aspirin has an antiplatelet effect and is therefore used at low but prolonged doses to prevent heart attacks, ischemic strokes and blood clots in high-risk people.

To coordinate metal cations, aspirin typically involves the carboxylate group, as exemplified by $\text{Cu}_2(\text{asp})_4$, which has demonstrated antioxidative properties.⁵ After the hydrolysis of aspirin, the resulting salicylic acid can coordinate to metal cations through the carboxylate and phenol/phenolate groups, yielding structurally different metal salicylates.⁶ The combination of metal cations, aspirin/salicylic acid and an $\text{N}_2\text{N}'$ -divergent ligand as a linker between metal cations offers the possibility of obtaining coordination polymers hosting the bioactive molecules. This type of strategy was used with several carboxylate-based drugs such as nonsteroidal anti-inflammatory drugs (NSAIDs): naproxen, ketoprofen, ketorolac, biotin, levodopa, indomethacin, carbocysteine,² ibuprofen^{2,7} and diclofenac.^{2,3}

We are interested in the preparation and study of organized solid-state materials based on coordination polymers containing a coordinated drug or active pharmaceutical ingredient

^aUniversidade de Vigo, Departamento de Química Inorgánica, Facultade de Química, 36310 Vigo, Spain. E-mail: alagobla@ull.edu.es

^bMetallosupramolecular Chemistry Group, Galicia Sur Health Research Institute (IIS Galicia Sur). SERGAS-UVIGO, Galicia, Spain

^cDepartamento de Química, Facultad de Ciencias, Sección Química Inorgánica, Universidad de la Laguna, 38206 La Laguna, Spain

^dServizo de Determinación Estructural, Proteómica e Xenómica, CACTI Universidade de Vigo, Spain



(API). In this way, we have previously explored the Zn(II)/ibuprofen/bis(4-pyridylthio)methane (SCS) system,⁷ finding that the resulting 1D polymeric material shows a high drug content and stability and that the N,N'-divergent ligand SCS is very useful for the preparation of such coordination polymers. More recently, Murphy and colleagues³ introduced the concept of Therapeutic Coordination Polymers (TCPs), non-porous coordination polymers that utilize metal-ligand interactions to achieve degradation-based drug release. Building on these works, we have considered exploring the incorporation of aspirin or salicylic acid in Zn(II)/Cu(II) coordination polymers facilitated by the linking role of SCS.

A bibliographic search on crystalline materials based on Zn(II) or Cu(II) coordination compounds with salicylate and an N,N'-divergent ligand yielded the information summarized in Table S1.^{8–12} From this information several observations can be drawn: (i) the compounds have been prepared by hydro/solvothermal or diffusion methodologies; (ii) when aspirin (acetylsalicylic acid, Hasp) is used as a reagent, hydrolysis occurs, and the resulting metal complex incorporates salicylate (Hsal[−]); (iii) the dimensionality of the metal complexes ranges from 0D to 2D, but the N,N'-divergent ligand does not always yield coordination polymers,^{8,10} and the salicylate (Hsal[−]) contributes to an increase in dimensionality in one case¹⁰; (iv) in all cases, the salicylate ligand uses the carboxylate group to coordinate the metal cations showing monodentate, chelating and bis-monodentate bridging coordination modes; and (v) in the Cu(II)/Hsal[−]/4,4'-bipy system,^{10,11} the synthesis by diffusion yields different molecular and polymeric crystalline species, showing that under very similar synthetic conditions, different metal complexes can be stabilized. These observations have aroused our interest in exploring the solid-state coordination chemistry of the Cu(II) and Zn(II)/aspirin and salicylic acid/bis(4-pyridylthio)methane (SCS) system using different synthetic methods to investigate the possibilities of obtaining various crystalline species. As a result, we report here the preparation and structural characterization of three polymorphic forms and a pseudopolymorph of a 1D Zn(II) coordination polymer, two 2D and one 3D Cu(II) coordination polymers, one organic cocrystal and one organic salt.

Results and discussion and experimental

Synthesis and characterization

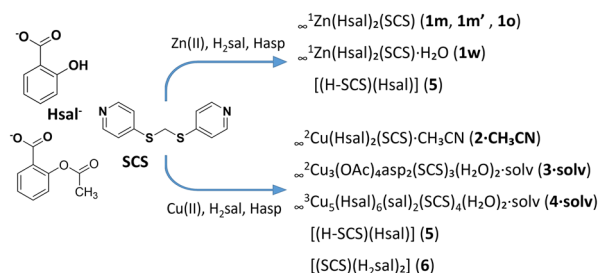
To study the reactivity of the Zn(II)/Cu(II)–SCS–salicylic/acetylsalicylic acid system, several synthetic methods were used: stirring at room temperature, heating under reflux, diffusion techniques, solvothermal conditions and reactions under microwave irradiation. Also, different metal cation precursors have been tested: for the Zn(II) compounds, ZnCl₂, ZnCO₃ and Zn(OAc)₂ salts and for the Cu(II) complexes, Cu(OAc)₂, CuCO₃, Cu(OH)₂ and the previously prepared Cu₂asp₄ (asp = acetylsalicylate/aspirinate).⁵ Most of the reactions were carried out in an

EtOH/H₂O mixture, except for those with Cu(II) performed under microwave irradiation using CH₃CN.

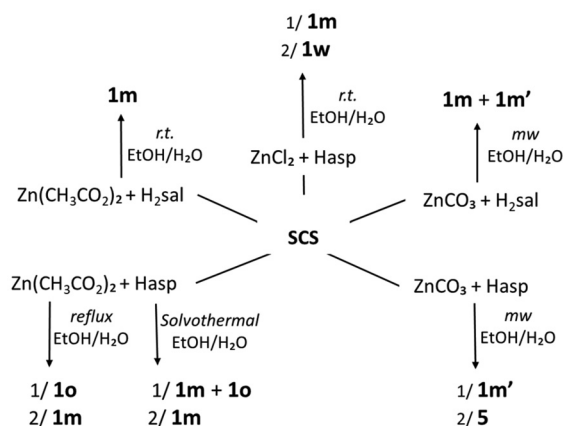
As a result of the synthetic work, the compounds listed in Scheme 1 have been isolated and characterized.

The resulting Zn(II) salicylate complexes are 1D polymers crystallized with different morphologies corresponding to three different polymorphs: two monoclinic forms (**1m** and **1m'**) and a third orthorhombic form (**1o**), and also the pseudopolymorph **1w** containing crystallization water. The isolated Cu(II) compounds are two salicylate coordination polymers (the 2D **2-CH₃CN** and the 3D **4-solv**) and the 2D aspirinate polymer **3-solv** which also contain a coordinated acetate anion. This last compound is the only one that contains an aspirinate ligand; in all other cases where acetylsalicylic acid or Cu₂asp₄ was used as a precursor, a deacetylation process occurred, producing a salicylate ligand.

Although simultaneous crystallization of the Zn(II) polymorphs is observed, some synthetic aspects can be highlighted. As shown in Scheme 2, the polymorph **1m** is obtained under all the synthetic conditions tested, showing that it is the more stable species. For the preparation of the polymorph **1m'**, the use of ZnCO₃ under microwave irradiation is required and in consequence, the key factor seems to be the metal salt. The polymorph **1o** was isolated only when Zn(CH₃CO₂)₂ and aspirin were used under reflux or solvothermal conditions,



Scheme 1 Compounds isolated from the reaction of SCS, H₂sal or Hasp and different zinc and copper salts.



Scheme 2 Synthetic procedures used in the study of the Zn(II)/SCS system.



suggesting that the combination of the two reagents is important. The pseudopolymorph **1w** has been isolated only once, in low yield, from a reaction using ZnCl_2 at room temperature, and again, the metal salt seems to be the key factor.

The synthetic results for the Cu(II) compounds (Scheme 3) show that the salicylate coordination polymers **2-CH₃CN** and **4-solv** consistently precipitate or crystallize simultaneously, regardless of the metal precursor or synthetic method used. For the crystallization of **2-CH₃CN**, the presence of CH_3CN is essential; even when the reaction is carried out in $\text{EtOH}/\text{H}_2\text{O}$, recrystallization in CH_3CN is required to obtain the crystalline material. Additionally, the synthetic conditions associated with the diffusion technique using Cu_2asp_4 appear to favour the crystallization of **4-solv**. The aspirinate coordination polymer **3-solv** was obtained in low yield only under microwave irradiation of a CH_3CN solution containing acetylsalicylic acid and $\text{Zn}(\text{CH}_3\text{COO})_2$, again indicating that the presence of CH_3CN is a determining factor in the crystallization process.

The salt $[(\text{H-SCS})(\text{Hsal})]$ (**5**) and the cocrystal $[(\text{SCS})(\text{H}_2\text{sal})_2]$ (**6**) have been obtained in the final phases of crystallization in several of the synthetic processes previously described (Schemes 2 and 3). Compound **5** resulted from the reaction of ZnCO_3 with aspirin and was also obtained, mixed with **6**, from the reaction of $\text{CuCO}_3\text{Cu}(\text{OH})_2$ with salicylic acid. Compound **6** crystallized from the medium of the reaction with Cu_2asp_4 that suffers decomposition and deacetylation of the coordinated aspirinate. Compounds **5** and **6** could also be crystallized, together from an $\text{EtOH}:\text{H}_2\text{O}$ solution of SCS and aspirin, and consecutively (first **6**, second **5**) from an $\text{EtOH}:\text{H}_2\text{O}$ solution of SCS and salicylic acid.

The diffractograms (XRD) of the compounds are in good agreement with the simulated patterns generated from single-crystal diffraction data (Fig. S4–S8).

The infrared spectra of the compounds (Fig. S1 and S2) present the characteristic bands of SCS, sometimes slightly displaced due to the coordination to the metal cations. The bands observed in the range $3400\text{--}3050\text{ cm}^{-1}$ are due to the OH vibrations from the hydroxyl groups and coordinated water molecules in compounds **3-solv** and **4-solv**. The spectra also

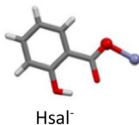
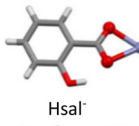
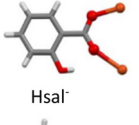

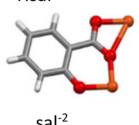
show bands close to 1600 cm^{-1} and between 1330 and 1390 cm^{-1} , attributable to $\nu_{\text{as}}(\text{OCO})$ and $\nu_{\text{s}}(\text{OCO})$, respectively. In compound **6**, the intense band at 1736 cm^{-1} (absent in the other compounds), assignable to the $\nu(\text{CO})$ vibration mode, agrees with the presence of salicylic acid (H_2sal). In the spectra of **2-CH₃CN** and **3-solv**, the weak band around 2300 cm^{-1} suggests the presence of CH_3CN in the second coordination sphere. In **5**, the broad band centered at 3370 cm^{-1} agrees with the presence of a protonated SCS pyridine in the salt.

The diffuse reflectance spectra (Fig. S3) of the Cu(II) compounds show broad bands between 640 and 680 nm attributable to d–d transitions, additional bands around 400 nm corresponding to ligand-to-metal charge transfer and bands between 309 and 323 nm due to intraligand transitions.

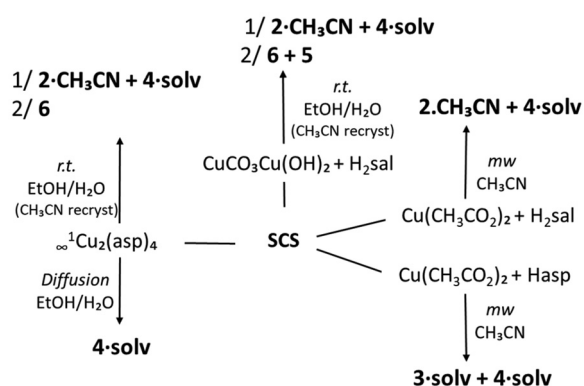
Crystal structures of polymers containing salicylate ($\text{Hsal}^-/\text{sal}^{2-}$) ligands

Crystal data and structure refinement parameters are reported in Tables S2 and S3, and selected bond lengths and angles are listed in Tables S4–S6. Table 1 shows the coordination modes adopted by the salicylate $\text{Hsal}^-/\text{sal}^{2-}$ ligands in the coordination polymers **1m**, **1m'**, **1o**, **1w**, **2-CH₃CN** and **4-solv**.

Table 1 Coordination modes of the salicylate ligands, coordination number and geometry around the metal, and M–O distances in the coordination polymers included in this work

Coordination modes $\text{Hsal}^-/\text{sal}^{2-}$	Compounds nc(M)/ coordination geometry	M–O distances (Å)
	1m , 1m' , 1o nc(Zn) = 4/ trigonal pyramidal (1m, 1m') nc(Zn) = 5/ square pyramidal (1o) 1w nc(Zn) = 4/trigonal pyramidal + tetrahedral 2-CH₃CN nc(Cu) = 5/ square pyramidal 4-solv nc(Cu) = 5/ square pyramidal	Zn–O _{carb_coord} : 1.940–1.995 Zn–O _{carb_uncoord} : 2.642–3.079 Cu–O _{carb_coord} : 1.949–2.088 Cu–O _{carb_uncoord} : 2.888–2.992
	1o nc(Zn) = 5/square pyramidal (1o) 4-solv nc(Cu) = 6/ octahedral	Zn–O _{carb_coord} : 2.121/2.263 Cu–O _{carb_coord} : 2.010/2.553
	4-solv nc(Cu) = 6/ octahedral	Cu–O _{carb_coord} : 1.946/2.325
	2-CH₃CN nc(Cu) = 5/ square pyramidal	Cu–O _{carb_coord} : 1.961 Cu–O _{carb_uncoord} : 2.888 Cu–O _{hydroxyl} : 2.345
	4-solv nc(Cu) = 6/ octahedral nc(Cu) = 5/square pyramidal	Cu–O _{carb_coord} : 1.922/1.946/2.538 Cu–O _{deprot_hydroxyl} : 1.893

O_{carb_coord} = coordinated carboxylate oxygen; O_{carb_uncoord} = uncoordinated carboxylate oxygen; O_{deprot_hydroxyl} = deprotonated hydroxyl.



Scheme 3 Synthetic procedures used in the study of the Cu(II)/SCS system.



Fig. 1 shows the 1D structures and metal coordination environments of the three polymorphic forms of ${}^1\text{Zn}(\text{Hsal})_2(\text{SCS})$ (**1m**, **1m'** and **1o**) and of the pseudopolymorph ${}^1\text{Zn}(\text{Hsal})_2(\text{SCS})\cdot\text{H}_2\text{O}$ (**1w**). ${}^1\text{Zn}(\text{Hsal})_2(\text{SCS})$ crystallizes in three different phases: the centrosymmetric prismatic **1m** and lamellar **1m'** crystals ($P2_1/c$) and the orthorhombic acentric non-polar **1o** ($P2_12_12_1$) phase. All the compounds are 1D coordination polymers due to the bridging role of the SCS ligand.

In **1m**, **1m'** and **1w**, the Zn cations are in an N_2O_2 environment, involving two nitrogen atoms of two bridging SCS ligands and two oxygen carboxylate atoms of two monodentate salicylate (Hsal^-) ligands (Table 1). The coordination geometry around the Zn cation can be evaluated using the τ_4 parameter¹⁵ so that a value of 1 corresponds to a regular tetrahedral (T_d) geometry, a value of 0 indicates a regular square-planar geometry (D_{4h}), and a value of 0.85 is due to a trigonal pyramidal geometry (C_{3v}). Compounds **1m** and **1m'** present τ_4 parameters of 0.88 and 0.89, respectively, indicating coordination geometries close to trigonal pyramidal. Compound **1w** presents two tetracoordinated Zn cations with coordination geometries slightly different: close to trigonal pyramidal around Zn1 ($\tau_4 = 0.87$) and close to tetrahedral around Zn2 ($\tau_4 = 0.92$). Compound **1o** presents the cation in an N_2O_3 environment with a monodentate Hsal^- and an anisobidentate chelating carboxylate of another Hsal^- ligand (Fig. 1). The geometry around the pentacoordinated cation can be evaluated through the τ_5 parameter¹⁶ ($\tau_5 = 0$, square pyramidal; $\tau_5 = 1$, trigonal bipyramidal), so a value of 0.22 indicates a distorted square pyramidal geometry. The polymorphism of ${}^1\text{Zn}(\text{Hsal})_2(\text{SCS})$ is due to the flexibility of the SCS ligand which adopts different conformations in each polymorph: GA in **1m**, AA in **1m'** and

G+G+ in **1o**. Fig. 1 illustrates this aspect by showing a superposition of the SCS ligands in the four polymers. In **1w**, ${}^1\text{Zn}(\text{Hsal})_2(\text{SCS})$ crystallizes including water in the lattice, and in this case, the SCS ligand presents two different conformations: GA and G+G+. The four 1D polymers present intra-chain hydrogen bonds (Tables S7 and S8) between the hydroxyl group and the uncoordinated oxygen atom of the carboxylate group of each salicylate ligand. In **1o**, the bidentate salicylate is also involved in hydrogen bonding with the hydroxyl group (Table S7). The packing of the chains of the four compounds is mainly due to C–H...O hydrogen bonds. In **1m'** and **1o**, the packing is reinforced by π – π interactions between the SCS pyridine rings with centroid–centroid distances of 3.546 and 3.493 Å, respectively. In **1w**, the water molecule in the second coordination sphere is mainly responsible for the packing, acting as a hydrogen donor and an acceptor between four chains. These interactions produce efficient packings as shown by the corresponding Kitaigorodskii packing indices:¹⁸ 71% for **1m** and **1m'**, 67% for **1o** and 72% for **1w**.

Fig. 2 and 3 show the 2D and 3D structures and the metal coordination environments of ${}^2\text{Cu}(\text{Hsal})_2(\text{SCS})\cdot\text{CH}_3\text{CN}$ (**2-CH₃CN**) and ${}^3\text{Cu}_5(\text{Hsal})_6(\text{sal})_2(\text{SCS})_4(\text{H}_2\text{O})_2$ (**4-solv**), respectively.

The 2D polymerization in **2-CH₃CN** is achieved by the coordination bridging role of the SCS and Hsal^- ligands (Fig. 2). The metal cation is coordinated to three oxygen atoms of three salicylate anions and to two nitrogen atoms of two molecules of SCS with a G+G+ configuration.¹⁷ The Addison parameter¹⁶ of 0.01 indicates a square-based pyramidal geometry. In the structure, each salicylate ligand behaves in a different way (Table 1): one acts as a terminal monodentate by the carboxylate group, while the other acts as a bis-monodentate bridge through the carboxylate and the hydroxyl groups. In the base of the pyramid, the Cu–O and Cu–N distances range between 1.949 and 2.022 Å, and at the apical position, occupied by the hydroxyl group, the distance increases to 2.345 Å. In the 2D structure, rectangular metalocycles are formed involving four Cu(II) cations, two SCS molecules and

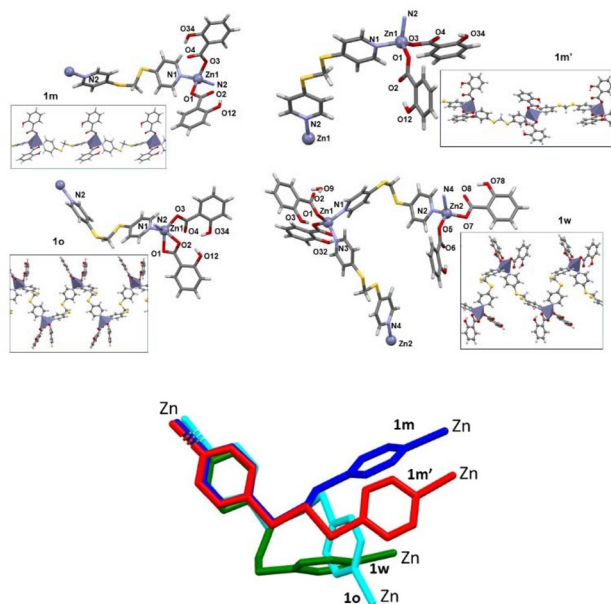


Fig. 1 Crystal structures and coordination environments of 1D polymers **1m**, **1m'**, **1o** and **1w** and superposition of the SCS ligand in the four polymers (bottom).

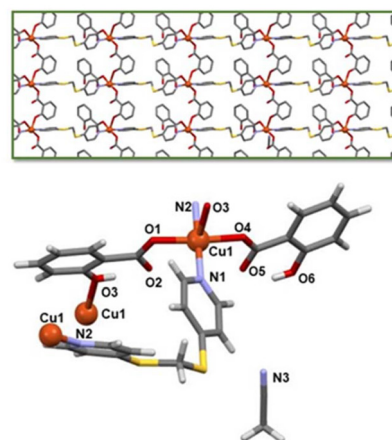


Fig. 2 Crystal structure and coordination environment of the 2D polymer **2-CH₃CN**.



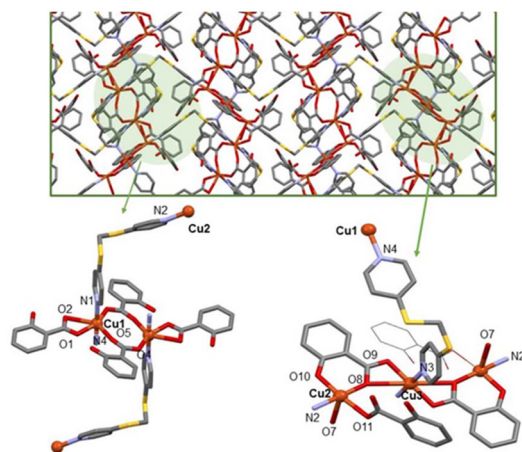


Fig. 3 Crystal structure and coordination environments of the 3D polymer **4-solv**. Hydrogen atoms are omitted to improve visualization.

two Hsal[−] ligands (Fig. 2) with Cu...Cu distances of 7.159 Å through the Hsal[−] ligand and 12.340 Å through the SCS ligand. As in the previously described 1D coordination polymers, the Hsal[−] ligands establish intramolecular OH...O_{carb} hydrogen bonds. The packing of the sheets involves the CH₃CN of crystallization through CH₃SCS...N (C...N distances between 3.501 and 3.730 Å) (Table S9) and CH(CH₃CN) ...π(Hsal[−] ring) (C...centroid distance, 3.550 Å) interactions. The packing is reinforced by the contribution of a π(SCS ring) ...π(Hsal[−] ring) interaction (centroid–centroid distance = 3.594 Å), leading to a Kitaigorodskii packing index¹⁸ of 66.7%.

The coordinative bridging role of the SCS, Hsal[−] and sal^{2−} ligands gives rise to the 3D coordination polymer **4-solv**. As shown in Table 1, the salicylate ligands take four different coordination modes: Hsal[−] acts as monodentate, bidentate chelate and bis-monodentate through the carboxylate group, and sal^{2−} acts as a bis-bidentate chelate bridging two metal centres (Fig. 3). The structure of **4-solv** is based on two types of metal nodes, Cu₂O₈ and Cu₃O₁₀, connected by SCS ligands. In the dinuclear Cu₂O₈ node (Fig. 3, left), the metal cations are in a distorted octahedral environment involving two oxygen atoms of a bidentate chelating Hsal[−], two oxygen atoms of a bis-monodentate bridging Hsal[−], and, at the axial positions, two nitrogen atoms of two SCS ligands. In the trinuclear Cu₃O₁₀ node (Fig. 3, right), the central metal cation (Cu3) is octahedrally coordinated by two SCS ligands and four carboxylate oxygen atoms belonging to two sal^{2−} ligands that coordinate also to two lateral metal cations (Cu2). These metal cations are in a square-pyramidal geometry (τ₅ = 0 (ref. 16)) based on two oxygen atoms (carboxylate and deprotonated hydroxyl groups) of the sal^{2−} ligand, one carboxylate oxygen atom of a monodentate Hsal[−] ligand, one water molecule and one SCS ligand. The SCS ligands connecting the nodes present two different conformations: GA and G+G⁺.¹⁷ The Kitaigorodskii packing index¹⁸ of 62.5% is lower than those calculated for the M/SCS/salicylate coordination polymers of lower dimensionality discussed above.

Crystal structure of the polymer containing aspirinate, ${}^2\text{Cu}_3(\text{OAc})_4\text{asp}_2(\text{SCS})_3(\text{H}_2\text{O})_2$ (**3-solv**)

3-solv is the only compound obtained with acetylsalicylate (asp[−]) coordinated without undergoing de-acetylation and the acetate ligand from the metal precursor. The 2D structure of this compound contains three different octahedral metal centres (Fig. 4). A planar Cu₂O₆ node, with four oxygen atoms belonging to two anisobidentate chelating acetate ligands and other two oxygen atoms of two bis-monodentate bridging acetate ligands, is connected by SCS ligands to two different octahedral Cu(II) centres (Cu2 and Cu3 in Fig. 4). The octahedral Cu2 center is coordinated by two anisobidentate chelating acetate ligands and two bridging SCS ligands at the axial positions. The Cu3 center is the only metal cation in the structure involved in the coordination to two monodentate acetylsalicylate (asp[−]) ligands. The octahedral environment around Cu3 is completed with two water molecules and two bridging SCS ligands (Fig. 4). All the SCS ligands in **3-solv** present the conformation G+G⁺.¹⁷ The highly disordered solvent component, which represents a potential solvent area of 723.3 Å³, could not be taken into account for the determination of the model and the Kitaigorodskii packing index¹⁸ under these conditions is 55.5%.

Crystal structure of the salt [(H-SCS)(Hsal)] (**5**) and the cocrystal [(SCS)(H₂sal)₂] (**6**)

Selected bond lengths and angles and hydrogen-bond distances are listed in Tables S6 and S10, respectively. The prismatic crystals of **5** and the needle-shaped crystals of **6** crystallize in the monoclinic *P*₂₁/*c* and the orthorhombic *P*₂₁2₁2₁ space groups, respectively. The structural resolution shows the ionic nature of **5** stabilized by the charge-assisted pyridinium-carboxylate N–H⁺...O[−] synthon and the neutral nature of **6**

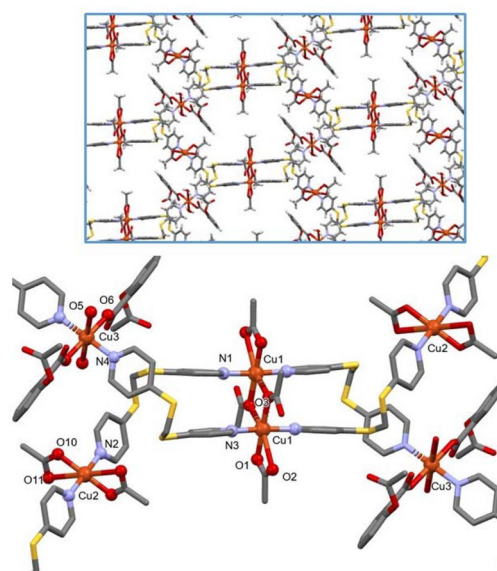


Fig. 4 Crystal structure and coordination environments of the 2D polymer **3-solv**. Hydrogen atoms are omitted to improve visualization.



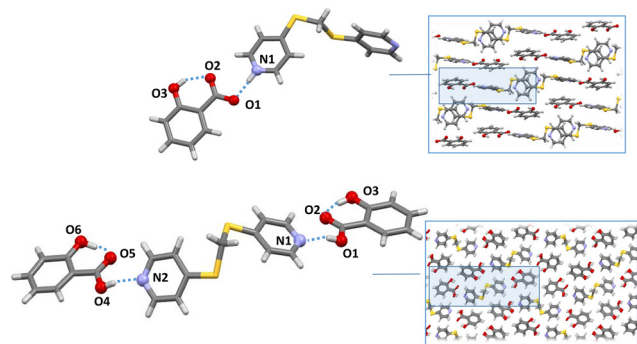


Fig. 5 Crystal structures of the salt **5** and the cocrystal **6**.

based on the O–H...N hydrogen bond synthon (Fig. 5). The stoichiometric ratio is 1 : 1 in **5**, involving the protonation of one of the two pyridyl groups of one SCS molecule in a GA conformation.¹⁷ The stoichiometry in **6** is 2 : 1 with the two pyridyl groups of one SCS molecule in a conformation G+G+¹⁷ involved in hydrogen bonds with two carboxylic groups of two salicylic acid molecules. The C–O bond length analysis allows differentiating between salt and the cocrystal.¹⁹ In **5**, a difference of 0.020 Å between the C–O distances agrees with the salt nature of the compound, and in **6**, the differences of 0.066 and 0.076 Å correspond to a cocrystal compound.

The packing of the salt **5** (Fig. 5) is mainly due to the contributions of the following interactions: CH_{py}...N_{unprotonated} (distance C...N = 3.327 Å), CH_{py}...π_{Hsal} (distance C...Hsal[−] centroid = 3.468 Å) and π(SCS ring)–π(SCS ring) with a distance between pyridine centroids of 3.602 Å. The packing of the cocrystal **6** (Fig. 5) is organized mainly by interactions involving the thioether sulfur atoms of SCS: OH...S (distance O...S = 3.220 Å), CH (methylene group of SCS)...S (distance C...S = 3.452 Å) and CH_{py}...S (distance C...S = 3.629 Å).

Thermal stability

The thermal stability of the compounds was investigated by thermogravimetric analysis (Fig. S11). Different thermal behaviours were observed for the unsolvated and the solvated compounds. In the solvated compounds **2**·CH₃CN, **3**·solv and **4**·solv, the first weight loss, at 150 °C, 130 °C and 100 °C, respectively, corresponds to the solvent loss. After this first step, the metal–organic framework begins its decomposition, which is completed around 300 °C. The unsolvated polymers are stable until 200 °C and a weight loss of around 68%, corresponding to the organic component, occurs between 200 °C and 400 °C.

Despite their different natures, ionic and neutral, compounds **5** and **6** present a similar thermal behaviour. Both compounds are stable up to 150 °C where their thermal degradation begins, which is completed at 350 °C.

Chemical stability

The ability of **1m** (1D), **3**·solv (2D), and **4**·solv (3D) to preserve their long-range ordered structure and release their com-

ponents under various chemical conditions was evaluated. The release of SCS or salicylate ligands was examined in water, acidic environments, and simulated physiological conditions using a phosphate-buffered solution (PBS, pH = 7.4).

Generally, the behaviour of copper compounds **3**·solv and **4**·solv was consistent across the different media tested, whereas the behaviour of the Zn compound **1m** was different. The supernatants of the solutions were analysed using UV-Vis spectroscopy after the compounds were immersed in water for 7, 14, and 21 days. No significant temporal differences were observed in the bands; however, the bands varied depending on the initial compound. A single band was observed for **1m** (275 nm) and **3**·solv (300 nm), while two bands were noted for **4**·solv (275 and 295 nm). These observations are likely associated with a higher concentration of SCS in the water solution of **1m** and a mixture of ligands in **4**·solv.

A similar behaviour was observed for **1m** when the study was conducted in PBS solution, with aliquots collected from 4 hours to 26 days, revealing a single band oscillating between 266–273 nm (Fig. S21). Conversely, **3**·solv and **4**·solv exhibited similar behaviours, with a band at 266 nm and two shoulders (at 240 and 296 nm) in the first 24 hours, which increased in intensity over time until the band at 295 nm became the most intense (approximately after 7 days). Ultimately, a single, intense band was observed at 272 nm. The PXRD pattern of water-treated **1m** indicates a transformation into a structure distinct from any of the polymorphs or salts isolated in this study (Fig. S14 and S15). The diffraction patterns of the solids remaining after water treatment of **3**·solv and **4**·solv demonstrate that both systems are crystalline and correspond to a pattern attributed to the same unidentified structure.

During the studies conducted in an acidic environment, it was observed that the pH stabilised in 30 minutes after the acid was introduced (Table S11). The behaviour was consistent across all compounds: the lower-intensity bands (ranging from 240–300 nm) shifted to bands of higher intensity and wavelength, specifically 312 nm when the pH was approximately 5 and 318 nm when the pH was approximately 3 (Fig. S16–S18). This behaviour is probably associated with an initial release of the SCS ligand, with a greater release of salicylic acid as the pH of the medium decreases. Regarding the solids resulting from these tests, **3**·solv exhibited considerable amorphous characteristics, **4**·solv retained good crystallinity, despite the inability to identify the phase, and the compound resulting from the acid treatment of **1m** exhibited the structure of [HSCS][ZnCl₄].⁷

In total, the analysis of the various UV-Vis spectra revealed the release of the SCS ligand and salicylic acid, as both combined bands or isolated SCS or salicylic bands were observed. However, the precise assignment of each analyte was not feasible due to the proximity and potential overlap of the bands. Additionally, these bands are likely to undergo bathochromic shifts upon protonation.⁷ The substantial differences in the release of ligands from these three compounds demonstrate the significant effect that structure and the metal ion could have on the release of salicylic acid from these materials.



These findings suggest the potential to modulate and control the presence of the bioactive molecule, salicylic acid, using the compounds developed in this study as drug carriers.

Cytotoxicity

The procedure followed for the cytotoxicity experiments is detailed in the SI. The cytotoxicity levels of polymorphs **1m** and **1w** were evaluated against both normal cells (MRC-5, non-tumour human fibroblasts) and tumour cells (NCI-H460, A549, and MDA-MB231). This comprehensive approach to testing allows for a thorough understanding of the compounds' effects on various cell types, providing crucial information about their selectivity and potential side effects.

The selection of these polymers for this study was based on several considerations: firstly, the drug content is notably high, with salicylic content of approximately 48 wt% in **1m**, **1m'**, and **1o**, and reaching 46 wt% in **1w**. Secondly, the structural simplicity is characterized by a lower number of components. Lastly, the synthetic procedure employed is notably straightforward, yielding higher outputs. The ability to efficiently synthesize these compounds in substantial quantities is crucial for guaranteeing large-scale production.

The cytotoxicity levels of **1m** and **1w** against normal cells (MRC-5, non-tumour human fibroblasts) were determined and compared with the SCS or ZnCl₂(SCS) compounds.⁷ The results of these experiments are included in Table S12. All the compounds exhibited low growth inhibition at the maximum concentration assayed ($10 \pm 3\%$ for 100 μM) and the growth inhibition curve was not calculated. These results suggest that the introduction of high concentrations of SCS and Zn compounds barely alters the cytotoxicity profile of SCS and Zn compounds on MRC-5 cells. The cytotoxicity of the polymeric compounds **1** and **1w** is related to the toxicity arising from the interactions between salicylic acid, the SCS ligand and Zn ions of the polymeric compounds with MRC-5 cells. The data obtained for compounds **1m** and **1w** were considered interesting for expanding cytotoxicity studies with three more cell lines.

The MTT assay was employed to evaluate the *in vitro* cytotoxicity of polymorphs **1m** and **1m'** and pseudopolymorph **1w** against multiple cancer cell lines, including MDA-MB-231 (triple-negative breast cancer) and A549 and NCI-H460 (lung cancer). The results of the MTT assay are presented in Table 2. While they were less cytotoxic than cisplatin, they showed cyto-

toxicity in all the tested cells. Notably, compound **1w** exhibits the highest cytotoxicity against all the tested cells. Within the series, **1w** showed almost double cytotoxicity effects in A549 cells, while all the compounds exhibited similar cytotoxicity against MDA-MB231 cells. These results could be very helpful for a thorough understanding of the crystal structure effects on various cell types, providing information about their selectivity and potential side effects.

The selective effect of the drug could be evaluated by comparing the cytotoxic activity of each compound against cancer and normal cells. The % growth inhibition suggests that compound **1w** could selectively target breast and lung cancer cells while exerting minimal effects on normal cells, as shown by the % growth inhibition observed with MRC-5. This is particularly relevant given that breast and lung cancers are among the most prevalent and clinically challenging cancers worldwide, underscoring the importance of developing effective therapeutic agents for these types.²⁰

Conclusions

The implementation of diverse synthetic methodologies within the Zn(II)/Cu(II)-SCS-salicylic/acetylsalicylic acid system enables the formation and isolation of multiple crystalline species, occasionally occurring simultaneously. This approach has yielded 1D Zn(II) coordination polymers, as well as 2D and 3D Cu(II) coordination frameworks, alongside the salt [(H-SCS)(Hsal)] and the cocrystal [(SCS)(H₂sal)₂]. In all metal complexes, the N,N'-divergent SCS ligand acts as a bridging unit, promoting 1D polymerization. Its conformational flexibility also accounts for the formation of three polymorphic forms of ¹Zn(Hsal)₂(SCS). In most cases, when aspirin or the Cu₂asp₄ complex was used as a reactant, a deacetylation process occurred, yielding salicylate ligands. Only in one instance was it possible to isolate the Cu(II) aspirinate compound ²Cu₃(CH₃CO₂)₄asp₂(SCS)₃(H₂O)₂. In these compounds, the salicylate ligands exhibit distinct coordination behaviours. The common monoanionic form, Hsal⁻, coordinates either to a single metal centre or bridges two metal ions, thereby contributing to the formation of coordination polymers. In contrast, the dianionic form, sal²⁻, binds to two metal centres through both carboxylate oxygen atoms and the phenoxide oxygen, facilitating the construction of a 3D coordination framework. Notably, the 3D polymer ³Cu₅(Hsal)₆(sal)₂(SCS)₄(H₂O)₂ incorporates both anionic forms of salicylate: Hsal⁻ adopts two distinct coordination modes, while sal²⁻ is responsible for driving the 3D polymerization. Compounds **1m**, **3-solv**, and **4-solv** demonstrated distinct release patterns of SCS and salicylate ligands in water, acidic environments, or simulated physiological conditions. These findings highlight the potential of these compounds as drug carriers for controlled release of bioactive molecules, specifically salicylic acid. Compounds **1m** and **1w** demonstrated low cytotoxicity against normal cells while exhibiting cytotoxic effects on various cancer cell lines. Notably, compound **1w** showed the highest cytotoxicity against

Table 2 Percentage of cell growth inhibition by 100 μM solutions of the zinc compounds

Compounds	Cell line		
	NCI-H460	A549	MDA-MB231
1m	35 \pm 1	28 \pm 1	43 \pm 2
1m'	35 \pm 1	26 \pm 2	42 \pm 1
1o	38 \pm 1	26 \pm 1	41 \pm 1
1w	50 \pm 2	44 \pm 1	47 \pm 1
Reference (cisplatin)	67 \pm 2	78 \pm 1	78 \pm 1



all tested cancer cells, with particularly strong effects on A549 lung cancer cells. These findings underscore the importance of the crystal structure in determining biological activity and pave the way for future research into the optimization and application of these zinc-based polymeric compounds in therapeutic applications.

Experimental

Materials and methods

The ligand bis(4-pyridylthio)methane (SCS) was prepared as described previously.²¹ The precursor ${}^1\text{Cu}_2\text{asp}_4$ (Hasp = aspirin) was prepared by reaction of $\text{Cu}(\text{CH}_3\text{CO}_2)_2 \cdot \text{H}_2\text{O}$ with acetylsalicylic acid in H_2O .^{13,14} The other starting materials and solvents were obtained commercially and used as supplied. Elemental analysis (C, H, N) was carried out on a Fisons EA-1108 microanalyser. Infrared spectra were recorded in the solid phase by ATR on a Jasco FT/IR-6100 spectrophotometer. Solid state and solution UV-vis spectra were recorded on a Jasco V670 spectrophotometer over the range of 1200–200 nm. TGA/DSC analysis profiles were obtained with the thermal analyser TGA-ATD/DSC, SETSYS Evolution 1750 (Setaram).

Synthesis and crystallization of the complexes

${}^1\text{Zn}(\text{Hsal})_2(\text{SCS})$ polymorphs **1m, **1m'** and **1o** and pseudopolymorph **1w**.** A simultaneous crystallization of the polymorphs is observed under the synthetic conditions tested (Scheme 2). We describe here the experimental procedures for the formation of a greater amount of each polymorph preferably as a single crystalline solid phase.

${}^1\text{Zn}(\text{Hsal})_2(\text{SCS})$ (1m**).** A mixture of 0.094 g (0.43 mmol) of $\text{Zn}(\text{OAc})_2 \cdot 2\text{H}_2\text{O}$, 0.101 g (0.43 mmol) of SCS and 0.125 g (0.91 mmol) of salicylic acid in 20 mL of $\text{H}_2\text{O}/\text{EtOH}$ (1 : 2) was stirred at room temperature for 24 h. The resulting white precipitate of **1m** was filtered off and dried under vacuum. Colourless single crystals of **1m** (*m* = monoclinic crystal system) were obtained by slow evaporation of the mother liquor.

Data for **1m**. Yield 37%. Anal. calcd for $\text{C}_{25}\text{H}_{20}\text{N}_2\text{O}_6\text{S}_2\text{Zn}$: N 4.9%, C 52.3%, H 3.5%. Found: N 4.9%, C 52.1%, H 3.5%. IR (cm^{-1}): 3062w, $\nu(\text{OH})$; 1629w, 1596s, $\nu_{\text{as}}(\text{OCO})$; 1564s, 1535w, 1483s, $\nu(\text{ring})$; 1393vs, $\nu_{\text{s}}(\text{OCO})$; 1255s, 1226m, 1208w, $\omega(\text{CH}, \text{CH}_2)$; 1025s (ring breathing); 769s, $\gamma(\text{CH})$; 705s, 639vs, $\nu(\text{C}-\text{S})$.

Single crystals of **1m** were also obtained from the reaction at room temperature of ZnCl_2 , acetylsalicylic acid and SCS in $\text{EtOH}/\text{H}_2\text{O}$.

${}^1\text{Zn}(\text{Hsal})_2(\text{SCS})$ (1o**)**

Method 1: reflux. A mixture of 0.094 g (0.43 mmol) of $\text{Zn}(\text{OAc})_2 \cdot 2\text{H}_2\text{O}$, 0.101 g (0.43 mmol) of SCS and 0.154 g (0.86 mmol) of acetylsalicylic acid in 20 mL of $\text{H}_2\text{O}/\text{EtOH}$ (1 : 2) was heated under reflux for 8 h. After 4 days, the evaporation of the resulting colourless solution yielded colourless cubic crystals of **1o** (*o* = orthorhombic crystal system, yield 49%). After 15 days of evaporation, single crystals of **1m** were also isolated.

Method 2: solvothermal. A mixture of a solution of 0.222 g (1.01 mmol) $\text{Zn}(\text{OAc})_2 \cdot 2\text{H}_2\text{O}$ in 5 mL H_2O and a suspension of 0.244 g (1.04 mmol) of SCS in 5 mL of EtOH was stirred for 30 minutes at room temperature. Then, a solution of 0.375 g (2.08 mmol) of acetylsalicylic acid in 5 mL EtOH was added. The resulting mixture with pH 5 was treated with NaOH 1 M until reaching pH = 7. The resulting suspension was sealed in a 20 mL Teflon-lined autoclave, heated to 120 °C for 3 days, and then slowly cooled to room temperature at a rate of 7 °C h^{-1} . The resulting crystalline white precipitate of **1m** and **1o** was filtered off and dried under vacuum. Some single crystals of **1m** were isolated by slow evaporation of the mother liquor.

Data for **1o**. Anal. calcd for $\text{C}_{25}\text{H}_{20}\text{N}_2\text{O}_6\text{S}_2\text{Zn}$: N 4.8%, C 52.3%, H 3.5%. Found: N 5.0%, C 51.9%, H 3.7%. IR (cm^{-1}): 3050w, $\nu(\text{OH})$; 1627w, 1594s, $\nu_{\text{as}}(\text{OCO})$; 1551m, 1537w, 1481m, $\nu(\text{ring})$; 1392s, $\nu_{\text{s}}(\text{OCO})$; 1250s, 1223m, 1154w, $\omega(\text{CH}, \text{CH}_2)$; 1024s (ring breathing); 751s, $\gamma(\text{CH})$; 702s, 668s, $\nu(\text{C}-\text{S})$.

${}^1\text{Zn}(\text{Hsal})_2(\text{SCS})$ (1m'**).** A mixture of 0.111 g (0.89 mmol) of ZnCO_3 , 0.202 g (0.86 mmol) of SCS and 0.126 g (0.91 mmol) of salicylic acid in 20 mL of $\text{EtOH}/\text{H}_2\text{O}$ (2 : 1) was irradiated for 10 min in a modified conventional microwave oven.²² After 3 days, the unreacted ligand and metal salt were filtered off and after 2 months, the resulting colourless solution yielded single crystals of **1m** (distorted cubic shape) and **1m'** (lamellar shape) which were separated manually.

Another synthetic option is the reaction under microwave irradiation (10 minutes) of 0.113 g (0.90 mmol) of ZnCO_3 , 0.204 g (0.87 mmol) of SCS and 0.161 g (0.89 mmol) of acetylsalicylic acid in 20 mL $\text{EtOH}/\text{H}_2\text{O}$ (1 : 1). After the filtration of the resulting suspension, the evaporation of the mother liquor (3 days) allowed the isolation of single crystals of **1m'** (47%). The evaporation of the remaining mother liquor for 15 days gave rise to the crystallization of $[(\text{H}-\text{SCS})(\text{Hsal})]$ (**5**).

Data for **1m'**. Anal. calcd for $\text{C}_{25}\text{H}_{20}\text{N}_2\text{O}_6\text{S}_2\text{Zn}$: N 4.9%, C 52.3%, H 3.5%. Found: N 5.3%, C 52.9%, H 3.5%. IR (cm^{-1}): 3360w, $\nu(\text{OH})$; 1627w, 1596m, $\nu_{\text{as}}(\text{OCO})$; 1567s, 1538w, 1482m, $\nu(\text{ring})$; 1392vs, $\nu_{\text{s}}(\text{OCO})$; 1254s, 1227m, 1190w, $\omega(\text{CH}, \text{CH}_2)$; 1025s (ring breathing); 755s, $\gamma(\text{CH})$; 705vs, 668vs, $\nu(\text{C}-\text{S})$.

${}^1\text{Zn}(\text{Hsal})_2(\text{SCS}) \cdot 1/2\text{H}_2\text{O}$ (1w**).** A mixture of a suspension of 0.065 g (0.48 mmol) of ZnCl_2 with 0.10 g (0.43 mmol) of SCS in 10 mL $\text{EtOH}/\text{H}_2\text{O}$ (2 : 1) and a solution of 0.083 g (0.46 mmol) of acetylsalicylic acid with 0.027 g (0.68 mmol) of NaOH in 10 mL of $\text{EtOH}/\text{H}_2\text{O}$ (2 : 1) was stirred at room temperature for 16 h. A white precipitate of **1m** (90%) was filtered off and dried under vacuum. The evaporation of the colourless mother liquor yielded single crystals of **1w** (8%).

Data for **1w**. Anal. calcd for $\text{C}_{25}\text{H}_{21}\text{N}_2\text{O}_{6.5}\text{S}_2\text{Zn}$: N 4.8%, C 51.6%, H 3.6%. Found: N 4.7%, C 50.8%, H 3.4%. IR (cm^{-1}): 3080w, $\nu(\text{OH})$; 1628m, 1597vs, $\nu_{\text{as}}(\text{OCO})$; 1562m, 1538w, 1483w, $\nu(\text{ring})$; 1390s, $\nu_{\text{s}}(\text{OCO})$; 1251vs, 1224m, 1192m, $\omega(\text{CH}, \text{CH}_2)$; 1024s (ring breathing); 753s, $\gamma(\text{CH})$; 701vs, 669vs, $\nu(\text{C}-\text{S})$.

Copper(II) complexes **2-CH₃CN**, **3-solv** and **4-solv**

${}^2\text{Cu}(\text{Hsal})_2(\text{SCS}) \cdot \text{CH}_3\text{CN}$ (2-CH₃CN**)**

Method 1: room temperature. A mixture of 0.190 g (0.23 mmol) of ${}^1\text{Cu}_2(\text{asp})_4$ ⁵ and 0.102 g (0.44 mmol) of SCS in



20 mL EtOH/H₂O (2 : 1) was stirred at room temperature for 24 h. After the filtration of the resulting suspension, the evaporation of the mother liquor produced a green crystalline material that was dissolved in 20 mL of CH₃CN/ⁱPrOH (1 : 1). The slow evaporation of this solution yielded a green solid corresponding to a mixture of **4-solv** and **2-CH₃CN**. The evaporation of the remaining solution produced colourless single crystals of [(SCS)(H₂sal)]₂ (**6**).

Also, at room temperature, by reaction of 0.083 g (0.38 mmol) of CuCO₃·Cu(OH)₂·0.5H₂O, 0.205 g (0.88 mmol) of SCS and 0.135 g (0.98 mmol) of salicylic acid in 30 mL EtOH/H₂O (2 : 1) a green precipitate was formed which after recrystallization in CH₃CN showed a diffractogram corresponding to a mixture of **4-solv** and **2-CH₃CN**. After filtration, the resulting colourless solution yielded colourless single crystals of **5** and **6**.

Method 2: microwave irradiation. A mixture of 0.095 g (0.476 mmol) of Cu(OAc)₂·H₂O, 0.100 g (0.427 mmol) of SCS and 0.137 g (1 mmol) of salicylic acid in 20 mL of CH₃CN was irradiated for 10 min in a microwave oven. Upon cooling, some single crystals of **4-solv** immediately formed, and after slow evaporation for 3 days, blue single crystals of **2-CH₃CN** were obtained (20%).

Data for **2-CH₃CN**. Anal. calcd for C₂₇H₂₃N₃O₆S₂Cu: N 6.9%, C 52.9%, H 3.7%. Found: N 6.6%, C 52.4%, H 3.2%. IR (cm⁻¹): 3070w, ν(OH); 2369w, ν(CN); 1625w, 1598s, ν_{as}(OCO); 1559m, 1540w, 1481s, ν(ring); 1389s, ν_s(OCO); 1254s, 1223m, 1193m, ω(CH, CH₂); 1026s (ring breathing); 755s, 728s, γ(CH); 703vs, 667vs, ν(C-S).

²Cu₃(OAc)₄asp₂(SCS)₃(H₂O)₂-**solv** (**3-solv**). A mixture of 0.094 g (0.471 mmol) of Cu(OAc)₂·H₂O, 0.102 g (0.435 mmol) of SCS and 0.154 g (0.854 mmol) of acetylsalicylic acid in 20 mL of CH₃CN was irradiated for 10 min in a modified conventional microwave oven. The evaporation for 6 days of the resulting blue solution yielded blue single crystals of **3-solv** (<20%). Complete evaporation of the resulting solution produced a blue oil that was dissolved in 10 mL of CH₃CN/ⁱPrOH (1 : 1); the evaporation of this solution yielded green single crystals of **4**.

Data for **3-solv**. Anal. calcd for C₄₃H₅₁N₇O₁₃S₄Cu₂ (solv = 3CH₃CN + 2H₂O): N 8.7%, C 45.8%, H 4.5%. Found: N 8.1%, C 45.9%, H 4.2%. IR (cm⁻¹): 3640, 3070w, ν(OH); 2324w, ν(CN); 1624w, 1596s, ν_{as}(OCO); 1559m, 1505w, 1483s, ν(ring); 1391m, ν_s(OCO); 1253vs, 1222m, ω(CH, CH₂); 2025s (ring breathing); 756s, γ(CH); 704s, 669s, ν(C-S).

³Cu₅(Hsal)₆(sal)₂(SCS)₄(H₂O)₂-**solv** (**4-solv**). To a suspension of 0.107 g (0.13 mmol) of ¹Cu₂(asp)₄ in 10 mL of H₂O placed in a test tube was slowly added 0.060 g (0.26 mmol) of SCS in 10 mL of EtOH. After 21 days of slow evaporation, small green single crystals of **4-solv** are formed.

Data for **4-solv**. Anal. calcd for C₁₀₀H₈₆N₈O₂₈S₈Cu₅ (solv = 2H₂O): N 4.6%, C 49.6%, H 3.5%. Found: N 4.6%, C 50.3%, H 3.5%. IR (cm⁻¹): 3060w, ν(OH); 1623w, 1596s, ν_{as}(OCO); 1560m, 1506w, 1482s, ν(ring); 1389s, ν_s(OCO); 1252s, 1221s, 1195s, ω(CH, CH₂); 1066m (ring breathing); 805s, 758vs, γ(CH); 703vs, ν(C-S).

Synthesis and crystallization of [(H-SCS)(Hsal)] (**5**) and [(SCS)(H₂sal)]₂ (**6**)

Compounds **5** and **6** crystallized in several of the synthetic processes described above. They can be prepared by the direct synthesis described below.

A solution of 0.202 g (0.86 mmol) of SCS and 0.160 g (0.89 mmol) of acetylsalicylic acid in 30 mL of EtOH/H₂O (1 : 2) was stirred for 48 h at room temperature. The slow evaporation of the resulting colourless solution yielded a mixture of single crystals of **5** and **6**.

Under the same conditions and solvent, but using a mixture of 0.207 g (0.88 mmol) of SCS and 0.13 g (0.94 mmol) of salicylic acid, the resulting colourless solution afforded single crystals of **6** (80%) after 1 month and single crystals of **5** (10%) after two weeks.

Data for **5**. Anal. calcd for C₁₈H₁₆N₂O₃S₂: N 7.5%, C 58.1%, H 4.3%. Found: N 7.5%, C 58.3%, H 4.5%. IR (cm⁻¹): 3370w,b, ν(NH); 3080w, ν(OH); 1608m, 1594m, ν_{as}(OCO); 1577s, 1538w (1481f, 1445d) ν(ring); 1363m, ν_s(OCO); 1257m, 1219m, 1197m, ω(CH, CH₂); 1028m (ring breathing); 764vs, γ(CH); 703vs, ν(C-S).

Data for **6**. Anal. calcd for C₂₅H₂₂N₂O₆S₂: N 5.5%, C 58.8%, H 4.3%. Found: N 6.1%, C 58.4%, H 4.1%. IR (cm⁻¹): 3030w, ν(OH); 1736m, ν(CO); 1582s, 1481s, 1446m, ν(ring); 1246s, 1217vs, ω(CH, CH₂); 1017s (ring breathing); 736vs, γ(CH); 697vs, ν(C-S).

Crystallography

Crystallographic data were collected at 100 K using a Bruker D8 Venture diffractometer with a Photon II CMOS detector and Mo-Kα radiation (λ = 0.71073 Å) generated by an Incoatec high-brilliance microfocus source equipped with Incoatec Helios multilayer optics. The software APEX3²³ was used for collecting frames of data, indexing reflections, and the determination of lattice parameters, SAINT²³ for integration of intensity of reflections, and SADABS²⁴ for scaling and empirical absorption correction. The structures were solved using a dual-space algorithm using the program SHELXT.²⁵ All non-hydrogen atoms were refined with anisotropic thermal parameters by full-matrix least-squares calculations on F² using the program SHELXL²⁶ with OLEX2.²⁷ Hydrogen atoms were inserted at calculated positions and constrained with isotropic thermal parameters. In **2-CH₃CN**, the crystal was twinned by inversion (BASF parameter, 0.350). In **3-solv** and **4-solv**, the OLEX2²⁶ solvent mask routine was used to remove the intensity contributions from the highly disordered solvent molecules. In **6**, one H₂sal molecule is disordered over two positions, and the site occupation factors were refined converging to 71 : 29. Drawings were produced with Mercury.²⁸ Special computations for the crystal structure discussion were carried out with PLATON.²⁹ Crystal data and structure refinement parameters are reported in Tables S2 and S3, where deposition reference numbers at the Cambridge Crystallographic Data Centre (CCDC) are also included. Selected bond lengths



and angles and hydrogen bond distances are listed in Tables S4–S10.

X-ray powder diffraction (PXRD) was performed using an X'pert Pro 3 (PANalytical) diffractometer with Cu-K α radiation ($\lambda = 1.5406 \text{ \AA}$) over the range 5 to 50° in steps of 0.026° (2 θ). The program MERCURY²⁷ was employed to obtain theoretical powder diffractograms from single crystal data. The program FULL PROF SUITE³⁰ and the tool WINPLOTR³¹ were used to perform profile matching.

Stability and degradation of the compounds

The stability and degradation of **1m**, **3-solv** and **4-solv** were investigated using UV-Vis and PXRD techniques. The samples were exposed to water for a duration of 21 days (Scheme S1), and their progression was monitored using UV-Vis at intervals of 7, 14, and 21 days. Under acidic conditions, 100 μL , 300 μL , and 1000 μL of 0.1 M HCl were added to the suspension of each compound (Scheme S2). These suspensions were stirred at room temperature for 24 hours, during which pH measurements were taken initially, after 30 minutes, and at the conclusion of the experiment (Table S11). Each compound (20 mg of **1m**, **3-solv** and **4-solv**) was immersed in 10 mL of 0.01 M PBS (phosphate-buffered solution) for 30 days in a sand bath maintained at 35–40 °C (Scheme S3). Changes were monitored through solution analysis by UV-Vis at 4 and 24 hours, and on days 5, 7, 8, 12, 13, 15, 19, and 26. UV spectrophotometry was conducted at room temperature in aqueous, acidic, or PBS solutions to confirm the presence of SCS or salicylate in solution. Two absorption bands were observed in the spectrum of salicylic acid in aqueous solution: a strong band at 320 nm and a weaker band at 252 nm. The absorption maximum of SCS was observed at 284 nm. The UV-Vis spectra of the polymeric compounds **1m**, **3-solv** and **4-solv** exhibited different bands depending on the media (see the SI). The PXRD patterns of the remaining solids after the various treatments were collected and compared with the theoretical patterns (SI).

Cytotoxicity assays

Cytotoxicity studies of some compounds were carried out on the MRC-5 (non-tumor human fibroblasts), NCI-H460 (human lung carcinoma), A549 (human lung carcinoma), and MDA-MB231 (human breast adenocarcinoma) cell lines obtained from the American Type Culture Collection (ATCC). The conditions of the experiments with cell lines are reported in Table S13.

Author contributions

Olaya Gómez-Paz: conceptualization, formal analysis, and investigation. Rosa Carballo: conceptualization, formal analysis, funding acquisition, methodology, and writing – original draft. Ana Belén Lago: formal analysis, investigation, and writing – original draft. Ezequiel M. Vázquez-López: conceptualization, formal analysis, funding acquisition, and writing – review. Berta Covelo: formal analysis, investigation, and

writing – review. All authors have read and agreed to the published version of the manuscript.

Conflicts of interest

There are no conflicts to declare.

Data availability

The data supporting this article have been included as part of the supplementary information (SI). Supplementary information: data and literature references regarding the crystal structures of Zn/Cu salicylate coordination polymers with *N,N'*-divergent ligands. Selected crystal data and structure refinement, selected bond lengths and angles, main hydrogen bonds, IR and UV-Vis-diffuse reflectance spectra and TGA curves of the complexes. Experimental procedure schemes, PXRD spectra and UV-Vis absorption spectra of the solutions for studies of stability in water, under acidic conditions and in PBS. Experimental conditions for the experiments with cell lines. See DOI: <https://doi.org/10.1039/d5dt02303c>.

CCDC 2487455–2487463 (**1m**, **1m'**, **1o**, **1w**, **2-CH₃CN**, **3-solv**, **4-solv**, **5** and **6**) contain the supplementary crystallographic data for this paper.^{32a–i}

Acknowledgements

This work was developed within the scope of the project ref. ED431C 2024/28 funded by Xunta de Galicia and ref. CNS2022-135453 funded by the MCIN/AEI/10.13039/501100011033 and by the “European Union NextGenerationEU”/PRTR. We thank the Structural Determination Service of the Universidade de Vigo-CACTI for X-ray diffraction measurements.

References

- 1 S. Kothawade and P. Shende, *Coord. Chem. Rev.*, 2024, **510**, 215851.
- 2 V. N. Vukotic, J. N. Murphy, J. Kobti and M. Dao, 2023, U.S. Patent and Trademark Office, filed on August 6th, 2021.
- 3 J. N. Murphy, J. L. Kobti, M. Dao, D. Wear, M. Okoko, S. Pandey and V. N. Vukotic, *Chem. Sci.*, 2024, **15**, 7041–7050.
- 4 J. R. Paterson and J. R. Lawrence, *J. Med.*, 2001, **94**, 445–448.
- 5 T. Fujimori, S. Yamada, H. Yasui, H. Sakurai and Y. T. Ishida, *J. Biol. Inorg. Chem.*, 2005, **10**, 831–841.
- 6 A. Gusev, Y. Baluda, E. Braga, M. Kryukova, M. Kiskin, E. Chuyan, M. Ravaeva, I. Cheretaev and W. Linert, *Inorg. Chim. Acta*, 2021, **528**, 120606.
- 7 A. B. Lago, A. Pino-Cuevas, R. Carballo and E. M. Vázquez-López, *Dalton Trans.*, 2016, **45**, 1614–1621.



- 8 S. Chooset, A. Kantacha, K. Chainok and S. Wongnawa, *Inorg. Chim. Acta*, 2018, **471**, 493–501.
- 9 Y.-Y. Liu, Y.-Y. Jiang, J. Yang, Y.-Y. Liu and J.-F. Ma, *CrystEngComm*, 2011, **13**, 6118–6129.
- 10 L.-G. Zhu and S. Kitagawa, *Inorg. Chem. Commun.*, 2003, **6**, 1051–1055.
- 11 L.-G. Zhu, S. Kitagawa, H. Miyasaka and H.-C. Chang, *Inorg. Chim. Acta*, 2003, **355**, 121–126.
- 12 S.-R. Zheng, X.-L. Wen, Z.-M. Liu, T. Xie, J.-B. Tan, J. Fan, S.-S. Hou and W.-G. Zhang, *Z. Anorg. Allg. Chem.*, 2014, **640**, 2057–2061.
- 13 B. Viossat, J.-C. Daran, G. Savouret, G. Morgant, F. T. Greenaway, N.-H. Dung, V. A. Pham-Tran and J. R. J. Sorenson, *J. Inorg. Biochem.*, 2003, **96**, 375–385.
- 14 N. Bouhmaida, M. A. Méndez-Rojas, A. Pérez-Benítez, G. Merino, B. Fraisse and N. E. Ghermani, *Inorg. Chem.*, 2010, **49**, 6443–6452.
- 15 L. Yang, D. R. Powell and R. P. Houser, *Dalton Trans.*, 2007, 955–964.
- 16 A. W. Addison, T. N. Rao, J. Reedij, J. van Rijn and G. C. Verschoor, *J. Chem. Soc., Dalton Trans.*, 1984, 1349–1356.
- 17 E. M. Page, D. A. Rice, K. Aarset, K. Hagen and R. J. Genge, *J. Phys. Chem. A*, 2000, **104**, 6672–6676.
- 18 A. I. Kitaigorodsky, *Molecular Crystals and Molecules*, Academic Press, New York, 1973, vol. 29.
- 19 S. L. Childs, G. P. Stahly and A. Park, *Mol. Pharm.*, 2007, **4**, 323–338.
- 20 I. Passi, L. M. Abraham, A. S. W. W. Raj, M. Varadhan, S. Muthuraman, M. P. Sivaramakrishnan, P. Vadivelu, R. Manoharan, M. Velusamy and V. Rajendiran, *Inorg. Chem.*, 2025, **54**, 14073–14090.
- 21 R. Carballo, B. Covelo, E. García-Martínez, A. B. Lago and E. M. Vázquez-López, *Z. Anorg. Allg. Chem.*, 2007, **633**, 780–782.
- 22 M. Ardon, P. D. Hayes and G. Hogarth, *J. Chem. Educ.*, 2002, **79**, 1249–1251.
- 23 Bruker, APEX3 and SAINT, Bruker AXS Inc., Madison, Wisconsin, USA, 2019.
- 24 L. Krause, R. Herbst-Irmer, G. M. Sheldrick and D. Stalke, *J. Appl. Crystallogr.*, 2015, **48**, 3–10.
- 25 G. M. Sheldrick, SHELXT – Integrated space-group and crystal structure determination, *Acta Crystallogr., Sect. A*, 2015, **71**, 3–8.
- 26 G. M. Sheldrick, Crystal Structure Refinement with SHELXL, *Acta Crystallogr., Sect. C*, 2015, **71**, 3–8.
- 27 O. V. Dolomanov, L. J. Bourhis, R. J. Gildea, J. A. K. Howard and H. Puschmann, *J. Appl. Crystallogr.*, 2009, **42**, 339–341.
- 28 C. F. Macrae, I. Sovago, S. J. Cottrell, P. T. A. Galek, P. McCabe, E. Pidcock, M. Platings, G. P. Shields, J. S. Stevens, M. Towler and P. A. Wood, *J. Appl. Crystallogr.*, 2020, **52**, 226–235.
- 29 A. L. Spek, *Acta Crystallogr., Sect. D: Biol. Crystallogr.*, 2009, **65**, 148–155.
- 30 J. Rodriguez-Carvajal, Commission on Powder Diffraction (CPD), 2001, 12–19.
- 31 T. Roisnel and J. Rodriguez-Carvajal, in Proceeding of the Seventh European Powder Diffraction Conference (EPDIC 7); 2000, pp. 118–123.
- 32 (a) CCDC 2487455: Experimental Crystal Structure Determination, 2025, DOI: [10.5517/ccdc.csd.cc2phdh3](https://doi.org/10.5517/ccdc.csd.cc2phdh3);
(b) CCDC 2487456: Experimental Crystal Structure Determination, 2025, DOI: [10.5517/ccdc.csd.cc2phdj4](https://doi.org/10.5517/ccdc.csd.cc2phdj4);
(c) CCDC 2487457: Experimental Crystal Structure Determination, 2025, DOI: [10.5517/ccdc.csd.cc2phdk5](https://doi.org/10.5517/ccdc.csd.cc2phdk5);
(d) CCDC 2487458: Experimental Crystal Structure Determination, 2025, DOI: [10.5517/ccdc.csd.cc2phdl6](https://doi.org/10.5517/ccdc.csd.cc2phdl6);
(e) CCDC 2487459: Experimental Crystal Structure Determination, 2025, DOI: [10.5517/ccdc.csd.cc2phdm7](https://doi.org/10.5517/ccdc.csd.cc2phdm7);
(f) CCDC 2487460: Experimental Crystal Structure Determination, 2025, DOI: [10.5517/ccdc.csd.cc2phdn8](https://doi.org/10.5517/ccdc.csd.cc2phdn8);
(g) CCDC 2487461: Experimental Crystal Structure Determination, 2025, DOI: [10.5517/ccdc.csd.cc2phdp9](https://doi.org/10.5517/ccdc.csd.cc2phdp9);
(h) CCDC 2487462: Experimental Crystal Structure Determination, 2025, DOI: [10.5517/ccdc.csd.cc2phdq6](https://doi.org/10.5517/ccdc.csd.cc2phdq6);
(i) CCDC 2487463: Experimental Crystal Structure Determination, 2025, DOI: [10.5517/ccdc.csd.cc2phdrc](https://doi.org/10.5517/ccdc.csd.cc2phdrc).

